

Current transport properties of SiO₂ films containing Ge nanocrystals

Minoru Fujii^{a)}

Department of Electrical and Electronics Engineering, Faculty of Engineering, Kobe University, Rokkodai, Nada, Kobe 657, Japan

Osamu Mamezaki

Division of Electrical and Electronics Engineering, The Graduate School of Science and Technology, Kobe University, Rokkodai, Nada, Kobe 657, Japan

Shinji Hayashi and Keiichi Yamamoto

Department of Electrical and Electronics Engineering, Faculty of Engineering, Kobe University, Rokkodai, Nada, Kobe 657, Japan

(Received 9 September 1997; accepted for publication 20 October 1997)

The electrical transport properties of SiO₂ films ($\geq 3 \mu\text{m}$ in thickness) containing Ge nanocrystals have been studied. We found that the films exhibit $T^{-1/2}$ dependence of $\ln(\sigma)$ under relatively low electric fields independent of the volume fraction of Ge in the films, where T and σ are the temperature and the conductivity, respectively. The observed electrical properties could be well explained by the theory developed by Šimánek [Solid State Commun. **40**, 1021 (1981)] which considers the tunneling of thermally activated carriers between neighboring nanocrystals. © 1998 American Institute of Physics. [S0021-8979(98)05303-1]

I. INTRODUCTION

Since the discovery of the highly efficient photoluminescence from porous-Si,¹ nanostructures of Si²⁻⁶ and Ge⁷⁻¹⁵ prepared by various methods have been the subject of intensive optical studies. Ge nanostructures have been prepared by implantation of Ge into SiO₂ films,⁷ cosputtering of Ge and SiO₂ and subsequent thermal annealing,⁸⁻¹² H₂ reduction of Si_xGe_{1-x}O₂ alloys,^{13,14} and oxidation of Si_xGe_{1-x} alloys.¹⁵ Although the preparation methods are different, all the films prepared have almost the same structure, i.e., Ge nanocrystals dispersed in SiO₂ matrices. These films are often reported to exhibit strong visible photoluminescence at room temperature^{7,10-15} and are expected to open up new possibilities for fabricating visible light emitting devices based on the Ge nanocrystals, although the mechanism of the visible photoluminescence has not been determined conclusively.

In order to realize various device applications including electroluminescent devices based on the Ge nanocrystals, detailed knowledge about the conduction properties of the systems consisting of Ge nanocrystals embedded in SiO₂ matrices is indispensable. However, despite the intensive optical studies, electrical properties of these systems have not been studied in detail.

In this work, we have studied electrical transport properties of the SiO₂ films containing Ge nanocrystals prepared by the cosputtering method. The SiO₂ films containing Ge nanocrystals may be modeled as three-dimensional resistance networks in which any site (Ge nanocrystal) is connected by a finite tunneling resistance onto its neighbors. If such films are very thin and only a few Ge nanocrystals are contained in a vertical direction, we can expect to observe the single-electron tunneling (SET) effects such as the Coulomb blockade and the Coulomb staircases due to the large

charging energies of the nanocrystals, and the resonant tunneling effects via quantized energy levels of the Ge nanocrystals. In the case of Ge nanocrystals a few nanometers in diameter, these effects are expected to be observable even at room temperature. On the other hand, if the films are very thick and a large number of Ge nanocrystals are contained in the vertical direction, the SET and resonant tunneling effects will be smeared out and cannot be observed explicitly, although these effects will implicitly affect the conduction properties of such films.

In this article, we report conduction properties of thick SiO₂ films ($\geq 3 \mu\text{m}$ in thickness) containing Ge nanocrystals. We have also studied the conduction properties of extremely thin films about 10 nm in thickness and observed the SET effects and the resonant tunneling effects. The results for the thin films will be published elsewhere. In this article, we first show the results of the high-resolution transmission electron microscopic (HRTEM) observations and demonstrate the formation of Ge nanocrystals in SiO₂ matrices. We will then show the results of electrical measurements. We will demonstrate that the present samples exhibit $T^{-1/2}$ dependence of $\ln(\sigma)$ at relatively low electric fields independent of the volume fraction of Ge nanocrystals in the films, where T and σ are the temperature and the conductivity, respectively.

II. EXPERIMENT

SiO₂ films containing Ge nanocrystals were prepared by a rf cosputtering method. Details of the preparation procedures are found in our previous articles.^{8,9} Small pieces of Ge chips ($5 \times 15 \text{ mm}^2$) were placed on a SiO₂ sputtering target 10 cm in diameter and they were cosputtered in Ar gas of 2.7 Pa. The purity of the Ge chips and the SiO₂ target were 99.9999% and 99.99%, respectively. During the deposition the substrates were not intentionally heated. For the as-deposited samples, no trace of crystallites was detectable

^{a)}Electronic mail: fujii@eedept.kobe-u.ac.jp

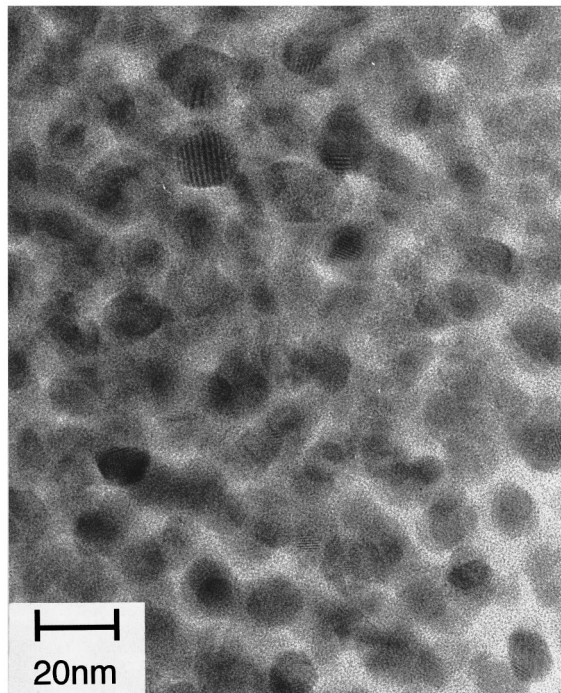


FIG. 1. Typical cross-sectional HRTEM image of a SiO₂ film containing Ge nanocrystals ($f_{\text{Ge}}=15.3\%$). Dark patches correspond to Ge nanocrystals.

by HRTEM observations and detectable Ge nanocrystals were grown only when the films were annealed. Thermal annealing was performed in vacuum of the order of 1×10^{-5} Pa at 800 °C for 30 min. In this method, the size of Ge nanocrystals can be controlled by changing the number of Ge chips during the cosputtering. The size (d) and the volume fraction of Ge nanocrystals (f_{Ge}) in the films were estimated by cross-sectional HRTEM (JEOL JEM-2010) observations and electron probe microanalyses (JEOL JXA-8900), respectively. The samples for the cross-sectional HRTEM observation were prepared by standard procedures including mechanical and ion thinning methods.

The substrates used were n^+ -Si wafers (0.005–0.018 Ω cm). After the cosputtering and the thermal annealing, upper and lower Al electrodes 5 mm in diameter were deposited. The dc current–voltage (I – V) and current–temperature (I – T) measurements in a vertical direction were made in a two terminal configuration by an Advantest R8340 electrometer. The measurements were performed in a temperature range between 20 and 300 K in a closed-cycle type He cryostat (Iwatani Cryomini) at the applied electric fields of up to 5×10^4 V/cm. Note that the current measured for the sample not containing Ge nanocrystals was smaller than 1×10^{-13} A for the temperature and the electric field range studied.

III. RESULTS

A. HRTEM observation

Figure 1 shows a typical cross-sectional HRTEM image of the SiO₂ film containing Ge nanocrystals ($f_{\text{Ge}}=15.3\%$). The dark patches seen correspond to Ge nanocrystals. We can see that the nanocrystals are randomly dispersed in the SiO₂ matrix. The enlarged image of Fig. 1 is shown in Fig. 2.

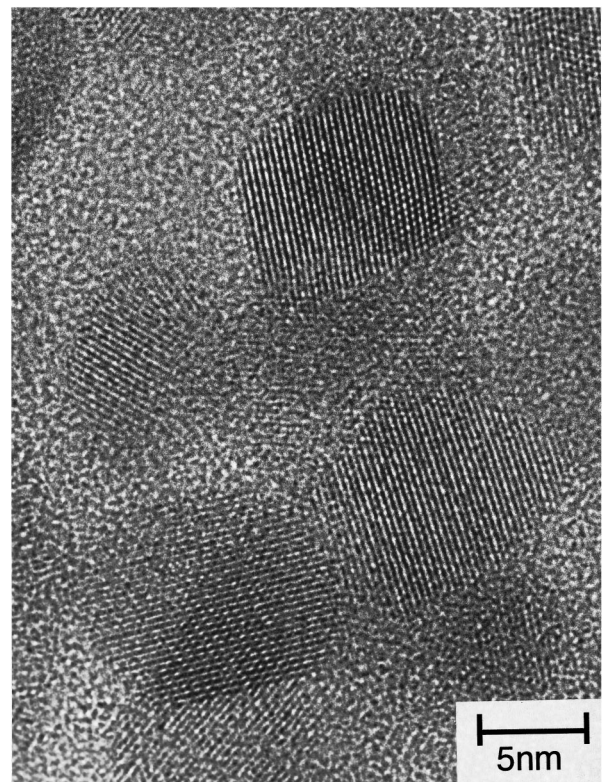


FIG. 2. Enlarged image of Fig. 1. Lattice fringes corresponding to the {111} planes of Ge nanocrystals with the diamond structure can clearly be seen. Ge nanocrystals are well dispersed in SiO₂ matrices.

Lattice fringes corresponding to the {111} planes of Ge crystals with the diamond structure can clearly be seen. The crystallinity of the nanocrystals is rather good. We can see that the nanocrystals are not aggregated and are isolated by SiO₂ layers. It should be noted here that, since the distances between the neighboring nanocrystals are a few nanometers as can be seen in Fig. 2, electrons can be transferred from one nanocrystal to another by tunneling. The volume fractions of Ge and the average diameters estimated from HRTEM images are summarized in Table I. We see that the average diameter increases as f_{Ge} increases.

B. Electrical measurements

Before discussing the electrical properties, it is important to distinguish between contact and bulk contributions. In the present work, we commonly observed rectification properties for the samples thinner than 1 μm , indicating that the contribution from contacts is non-negligible. In order to separate the bulk properties from contact ones, we increased the sample thickness until the rectification behavior disappears

TABLE I. Volume fractions of Ge (f_{Ge}), average diameters (d), and activation energies (T_0) obtained from Fig. 4.

$f_{\text{Ge}}(\%)$	d (nm)	T_0 (K)
4.2	3.8	197 465
8.8	5.6	192 774
15.3	8.9	108 129

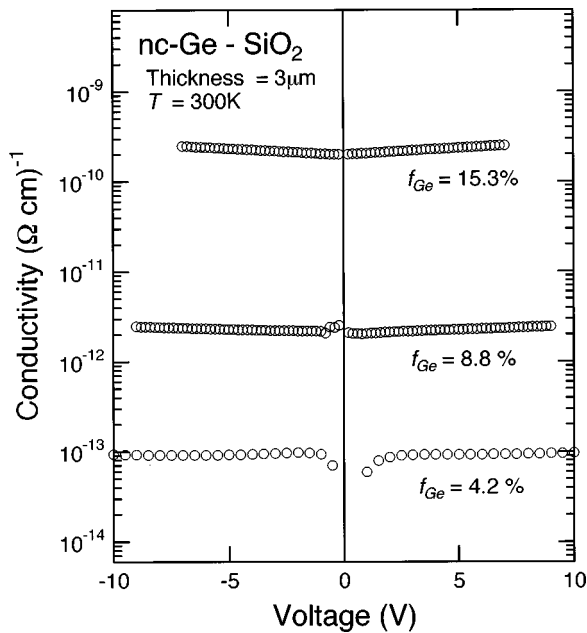


FIG. 3. Logarithmic conductivity of SiO_2 films containing Ge nanocrystals as a function of applied voltage for the samples with three different f_{Ge} . The conductivity is almost independent of the applied voltage.

on the data. Figure 3 shows conductivity (σ) versus voltage characteristics obtained for the samples with three different f_{Ge} . The thickness of the films was $3 \mu\text{m}$. We can see nearly symmetric σ - V characteristics. This suggests that the sample is sufficiently thick, enabling us to discuss the bulk properties. In order to confirm this fact, we compared I - V curves for the samples with two different thickness (3 and $5 \mu\text{m}$) and found that σ versus electric field relation was almost independent of the film thickness. This also implies that the contribution from contacts is negligible and we can study net conduction properties of the films if the thickness is larger than $3 \mu\text{m}$.

In Fig. 3, we can see that σ is nearly independent of the applied voltage and is very sensitive to f_{Ge} . As f_{Ge} increases from 4.2% to 15.3% , σ increases by several orders of magnitude. This systematic increase in σ indicates that the conduction in the present samples is governed by the Ge nanocrystals in SiO_2 matrices.

In order to study conduction mechanism, it is convenient to plot logarithm of the conductivity [$\ln(\sigma)$] as a function of $T^{-1/a}$, and find a proper value of a which straighten out experimental curves. We have studied the temperature dependence of the conductivity and first tried to plot $\ln(\sigma)$ as a function of T^{-1} ($a=1$, Arrhenius plot). However, the Arrhenius plot did not give a single straight line. This means that carriers are not simply activated to a mobility edge above which extended states exist. To find a proper value of a , we numerically fitted the experimental results and tried to find a . The values of a were around 2 independent of the applied field and f_{Ge} . Figure 4 shows $\ln(\sigma)$ plotted as a function of $T^{-1/2}$ for the samples with three different f_{Ge} at the applied field of $2 \times 10^4 \text{ V/cm}$. The solid lines are the results of the least squares fitting by straight lines. We can see that the observed σ can be fitted very well with the

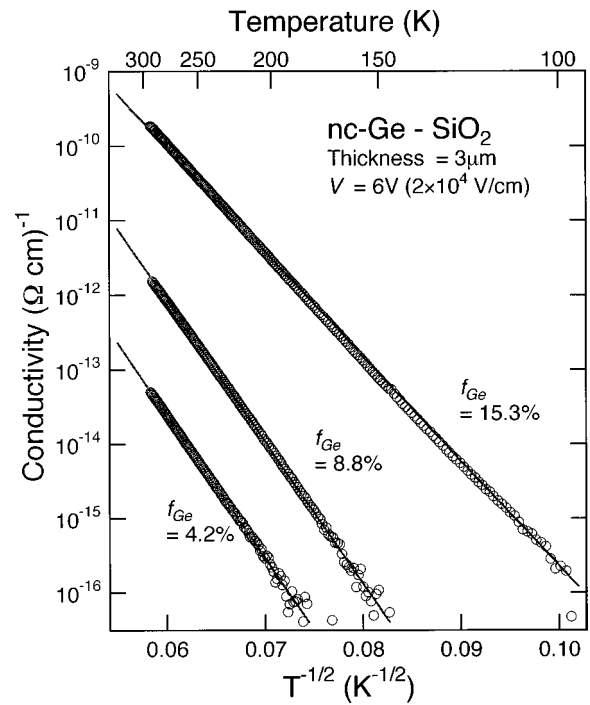


FIG. 4. Conductivity σ (in logarithmic scale) as a function of $T^{-1/2}$ for the samples with three different f_{Ge} . Solid lines are the results of the least squares fitting. For the easier comparison the top axis has the corresponding temperature scale.

straight lines. We can also find that the slope (T_0) of the $\ln(\sigma) \propto T^{-1/2}$ lines decreases as f_{Ge} increases. The values of T_0 estimated from Fig. 4 are summarized in Table I. It should be noted that T_0 was independent of the applied voltage and the film thickness, and depended only on f_{Ge} .

IV. DISCUSSION

A. Theories predicting the $\ln(\sigma) \propto T^{-1/2}$ relation

The relation of $\ln(\sigma) \propto T^{-1/2}$ at low electric fields has commonly been observed for metal-insulator composite films independent of the kinds of metals and insulators.¹⁶⁻¹⁹ In the metal-insulator composite films with relatively low metal concentration, metal particles are dispersed in insulating matrices. The structure is thus very similar to the present samples. In these films, $\ln(\sigma) \propto T^{-1/2}$ relation has been observed for a wide range of a volume fraction of metal particles. The slope of the $\ln(\sigma) \propto T^{-1/2}$ relation depends on the volume fraction of metal particles and decreases as the volume fraction increases. These films are also known to exhibit characteristic I - V curves. At high-electric fields, $\ln(\sigma)$ is proportional to the inverse of the applied voltage, while at low-electric fields, σ becomes independent of the applied voltage.¹⁶

To derive the $\ln(\sigma) \propto T^{-1/2}$ relation of the metal-insulator composite films, many theoretical considerations were made so far.¹⁶⁻¹⁹ In all the theoretical treatments, the current transport was considered on the basis of the thermally activated electron tunneling between metal particles. Abeles *et al.*¹⁶ proposed that the origin of the activation energy necessary to transfer an electron from one nanocrystal to another is the electrostatic charging energies of particles

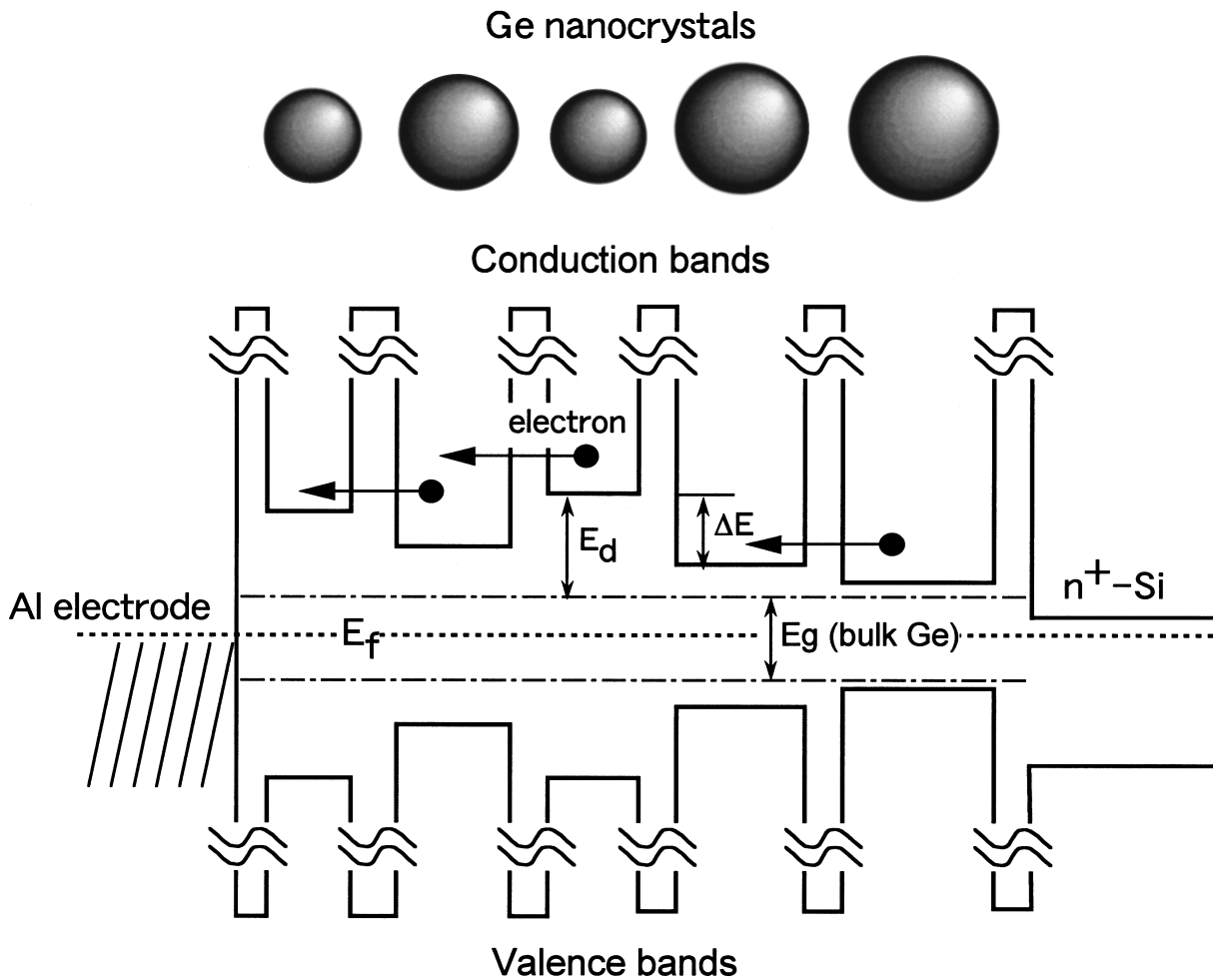


FIG. 5. Illustration of Ge nanocrystals connected via SiO_2 barriers, and the corresponding band diagram at zero bias. E_d represents the degree of high-energy shift of the conduction band edge, ΔE represents the difference of the conduction band edge between the neighboring nanocrystals.

(E_c). They derived the $\ln(\sigma) \propto T^{-1/2}$ relation under the assumption that the ratio of the particle diameter (d) and the particle separation (s) is constant throughout a sample. The theory is criticized by Šimánek.¹⁷ He pointed out that the theory fails to explain the observed $\ln(\sigma) \propto T^{-1/2}$ relation in a wide enough temperature range. The theory developed by Šimánek regards s as a random variable essentially uncorrelated with the particle diameter, because the shape of the particles is not perfectly spherical and the protrusions on the surface of the particles are expected to produce strong fluctuations in the effective local spacing. Furthermore, as the origin of the activation energy they considered not only the charging energy but also the distribution of the quantized energy levels of particles resulting from the fluctuation of the particle size. Assuming uniform distributions of the activation energies and the tunneling distances, they derived the $\ln(\sigma) \propto T^{-1/2}$ relation by means of the percolation method. Similar approach was used by Sheng and Klafter.¹⁸ They assumed a nonuniform distribution of the activation energy, and also derived the $\ln(\sigma) \propto T^{-1/2}$ relation by the percolation method.

Another class of theory which predicts the $\ln(\sigma) \propto T^{-1/2}$ relation is the variable range hopping conduction with a Coulomb gap derived by Efros and Shklovskii²⁰ for impurity

doped semiconductors. However, the model has been considered to be inappropriate in explaining the conduction properties of metal-insulator composite films.¹⁷⁻¹⁹

B. Comparison between experiment and theory

1. Conduction model

The conduction properties in the present samples are very similar to those of the metal-insulator composite films. First, both of them show the $\ln(\sigma) \propto T^{-1/2}$ relation under low-electric fields. Second, T_0 decreases as the volume fraction of conductive species increases. Third, the conductivity is nearly constant under low-electric fields. From the similarities of the conduction properties and the sample structures, i.e., conductive particles are dispersed in insulating matrices, we can expect the similar conduction mechanism for the SiO_2 films containing Ge nanocrystals and the metal-insulator composite films.

Figure 5 is the schematic drawing of the structure of the samples along the direction of a current flow, where Ge nanocrystals are separated each other by thin SiO_2 barriers. Corresponding energy band diagram at zero bias is also shown. It should be noted that the band gap of nanocrystals is widened by the zero-dimensional quantum confinement

effects and the degree of the widening depends on the size. Since the SiO₂ barriers are very thin, electrons can be transferred from one nanocrystal to another by tunneling as schematically shown in Fig. 5.

In the case of metal particles, the activation energy necessary for tunneling between neighboring particles is mainly the electrostatic charging energy of particles (E_c).¹⁶ Assuming that a particle is surrounded by many particles, the charging energy of the particle is expressed as¹⁶

$$E_c = \frac{e^2}{4\pi\epsilon\epsilon_0 d} \frac{(s/d)}{(1/2 + s/d)}, \quad (1)$$

where ϵ is the dielectric constant of SiO₂ matrices (≈ 3.9), ϵ_0 is the permittivity in vacuum, and s is the distance between the particle and the surrounding particles. In the case of the semiconductor nanocrystals, we also have to take into account the discreteness of the energy levels, because the degree of the size quantization for semiconductors is expected to be larger than that of metals.²¹ The degree of the high-energy shift of the conduction band edge (E_d) from the bulk edge due to the size quantization can be roughly estimated by the effective mass approximation as

$$E_d = \frac{\hbar^2 \pi^2}{2m_e^* (d/2)^2}, \quad (2)$$

where m_e^* is the effective mass for electrons. Taking the transversal and longitudinal effective masses at L point as $m_t^* = 0.082m_0$ and $m_l^* = 1.58m_0$, m_e^* can be estimated as $0.12m_0$ using $1/m_e^* = 1/3(1/m_t^* + 2/m_l^*)$.¹⁰ Since the present samples have a size distribution, E_d varies from one nanocrystal to another. This results in the energy difference of the conduction band edge between the neighboring nanocrystals (ΔE). The definitions of E_d and ΔE are shown in Fig. 5. In the following, we will assume that the activation energy necessary for the tunneling is the sum of E_c and ΔE .

As described above, two types of theories are developed in accounting for the $\ln(\sigma) \propto (T_0/T)^{1/2}$ relation of the metal-insulator composite films. The one assumes particular correlation between particle size and local separation between particles.¹⁶ The other does not make any assumption on them.^{17,18} Since we did not find any particular correlation between the size and the local separation in the HRTEM observations, we will consider the latter theories. In these theories, the metal-insulator composite films are modeled as the three-dimensional resistance networks in which any site (nanocrystal) is connected by a finite tunneling resistance onto its neighbors. This model is very much suitable for the present samples because Ge nanocrystals in the present samples are separated each other by SiO₂ tunneling barriers as can be seen in HRTEM images, and the current transport is considered to be made by the tunneling of electrons between the neighboring nanocrystals. We adopt the theory developed by Šimánek¹⁷ and quantitatively compare the experimental results with the theory. Assuming a uniform distribution of the particle separations and the activation energies, he derived $\ln(\sigma) \propto (T_0/T)^{1/2}$ relation using the percolation approach. The expression of T_0 is

$$T_0 = \frac{2P_c s_{\max} E_{\max}}{k_B \alpha}, \quad (3)$$

where P_c is the percolation threshold, s_{\max} is the maximum separation of particles in the current path, E_{\max} is the maximum value of the activation energy for the intergrain tunneling, and α is the effective decay length for the wave functions of electrons in the insulating region.

2. Comparison between experiment and theory

Although the Šimánek's model is very simple, it is possible to roughly estimate T_0 using Eq. (3) and compare the results with experimental ones at the order-of-magnitude level. To estimate T_0 from Eq. (3), the maximum separation of neighboring nanocrystals (s_{\max}) and the maximum activation energies (E_{\max}) in a current path are required. Since the precise information on the actual current path is not available, we roughly estimate s_{\max} as 3 nm from HRTEM images. We also assume that the activation energy becomes maximum when electrons are transferred from the largest to the smallest nanocrystals in the size distribution. In the case of the sample with $f_{\text{Ge}} = 15.3\%$, the smallest nanocrystal we found from HRTEM images was about 4 nm and the largest one was about 15 nm. Using Eq. (2), E_d of the 4 and 15 nm particles can be calculated to be 0.78 and 0.06 eV, respectively. The energy difference (ΔE_{\max}) is thus 0.72 eV. From Eq. (1), the charging energy necessary to add an electron to a nanocrystal 4 nm in diameter ($E_{c_{\max}}$) is 0.06 eV, if the particle is surrounded by many particles with the separation of 3 nm. Assuming that E_{\max} is the sum of ΔE_{\max} and $E_{c_{\max}}$, E_{\max} for the sample with $f_{\text{Ge}} = 15.3\%$ becomes 0.78 eV. It should be noted here that ΔE_{\max} of the present samples is much larger than $E_{c_{\max}}$. This is opposite to the case of the metal-insulator composite films, in which the effect of the charging energy is much more important and the intragrain level splitting is negligible.¹⁶

In order to estimate T_0 , we need the value of the percolation threshold P_c . Since P_c of the present samples is unknown, we adopt that of the simple cubic lattice of particles. In this case P_c becomes 0.25.²² Assuming $\alpha = 0.1$ nm¹⁷ and $E_{\max} = 0.78$ eV, T_0 becomes 136 000 K. This value is in good agreement with the experimental results shown in Table I, indicating that the conduction properties of the present samples can be well explained by the Šimánek's theory. It should be noted here that the observed T_0 in the present samples is very large and the large T_0 cannot be explained without taking into account ΔE .

As can be seen in Fig. 4 and Table I, T_0 increases as f_{Ge} decreases. From Eq. (3), the increase in T_0 is caused by the increases of s_{\max} and/or E_{\max} with decreasing f_{Ge} . We have studied the samples with a wide range of f_{Ge} by HRTEM and found that the average separation of nanocrystals is not so sensitive to f_{Ge} , provided that the annealing condition is the same. On the other hand, the average diameter depends strongly on f_{Ge} as can be seen in Table I. Since E_c and E_d are proportional to d^{-1} and d^{-2} , respectively, the reduction of the size causes significant increases in E_c and E_d . ΔE is also considered to increase significantly, because E_d becomes very sensitive to the size as the size decreases. There-

fore, we believe that the observed increase in T_0 is caused by the decrease in the size of Ge nanocrystals with decreasing f_{Ge} .

In the present work, I - V characteristics were nearly Ohmic (σ is nearly constant) as shown in Fig. 3. In the case of metal-insulator composite films, σ is nearly constant at low electric fields and at high electric fields, $\ln(\sigma)$ is proportional to the inverse of the applied field. We tried to measure the conduction at high electric fields. However, the present samples were vulnerable and the maximum electric field we could apply was 5×10^4 V/cm. In this electric field range, the conductivity was almost constant.

3. Conduction properties of SiO₂ films containing Ge clusters

In our previous work,²³ we have studied I - T characteristics of Si, Ge, or C doped SiO₂ films prepared by cosputtering of Si, Ge, or C with SiO₂ (without any thermal treatment). We demonstrated that these films generally exhibit a $T^{-1/4}$ dependence of $\ln(\sigma)$. Since previous optical studies for these films indicated that they are the systems of Si, Ge, or C clusters much smaller than 2 nm dispersed in SiO_x matrices,^{8,24-26} the conduction is considered to be mediated by the electronic states associated with the clusters distributed in the films.

The results of the present work demonstrate that the I - T characteristics of the films change from $\ln(\sigma) \propto T^{-1/4}$ to $\ln(\sigma) \propto T^{-1/2}$ relation as the clusters grow to nanocrystals several nanometers in diameter by the thermal annealing. In a previous theoretical work for the metal-insulator composite films, the crossover of $\ln(\sigma) \propto T^{-1/2}$ and $\ln(\sigma) \propto T^{-1/4}$ is predicted.¹⁸ It was suggested that the temperature at which the crossover occurs depends on the particle size. As the size decreases (activation energy increases), the temperature region of the $\ln(\sigma) \propto T^{-1/4}$ extends and this becomes a better overall fit than $T^{-1/2}$. On the other hand, increasing the grain size (decreasing the activation energy) has the effect of extending the $T^{-1/2}$ region to lower temperature. Therefore, the observed change from $\ln(\sigma) \propto T^{-1/4}$ relation to $\ln(\sigma) \propto T^{-1/2}$ relation by the thermal annealing may be explained by the decrease of the activation energy due to the growth of the nanocrystals.

V. SUMMARY

In summary, we have studied electrical transport properties of SiO₂ films containing Ge nanocrystals. We found that the present samples exhibit the $T^{-1/2}$ dependence of $\ln(\sigma)$ at relatively low electric fields for a wide range of the volume fraction of Ge nanocrystals. We also found that as the volume fraction of Ge nanocrystals increases, the slope of the $\ln(\sigma) \propto T^{-1/2}$ relation decreases. From the conduction properties and sample structures, we concluded that carrier transport in the present samples is carried out via Ge nanocrystals

by tunneling between adjacent nanocrystals. The activation energies obtained from I - T characteristics were in good agreement with that estimated by the Šimánek's theory. It was found that not only the charging energy but also the distribution of the quantized conduction band edge between the nanocrystals play significant roles in determining the conduction properties. We observed very similar conduction properties for SiO₂ films containing Si nanocrystals. The results will be published elsewhere.

ACKNOWLEDGMENTS

The authors are grateful to M. Kayahara for his valuable assistance in the experiment. This work was supported by a Grant-in-Aid for Scientific Research, from the Ministry of Education, Science, Sports and Culture, Japan, and a grant from the Takayanagi Foundation for Electronics Science and Technology.

- ¹L. T. Canham, Appl. Phys. Lett. **57**, 1046 (1990).
- ²H. Takagi, H. Ogawa, Y. Yamazaki, A. Ishizaki, and T. Nakagiri, Appl. Phys. Lett. **56**, 2379 (1990).
- ³H. Morisaki, F. W. Ping, H. Ono, and K. Yazawa, J. Appl. Phys. **70**, 1869 (1991).
- ⁴K. A. Littau, P. J. Szajowski, A. J. Muller, A. R. Kortan, and L. E. Brus, J. Phys. Chem. **97**, 1224 (1993).
- ⁵Y. Kanzawa, M. Fujii, S. Hayashi, and K. Yamamoto, Solid State Commun. **100**, 227 (1996).
- ⁶Y. Kanzawa, T. Kageyama, S. Takeoka, M. Fujii, S. Hayashi, and K. Yamamoto, Solid State Commun. **102**, 533 (1997).
- ⁷K. S. Min, K. V. Shcheglov, C. M. Yang, H. A. Atwater, M. L. Brongersma, and A. Polman, Appl. Phys. Lett. **68**, 2511 (1996).
- ⁸M. Fujii, S. Hayashi, and K. Yamamoto, Jpn. J. Appl. Phys., Part 1 **30**, 687 (1991).
- ⁹M. Fujii, M. Wada, S. Hayashi, and K. Yamamoto, Phys. Rev. B **46**, 15 930 (1992).
- ¹⁰Y. Maeda, Phys. Rev. B **51**, 1658 (1995).
- ¹¹L. Yue and Y. He, J. Appl. Phys. **81**, 2910 (1997).
- ¹²M. Zacharias, R. Weigand, B. Dietrich, F. Stolze, J. Bläsing, P. Veit, T. Drüsedau, and J. Christen, J. Appl. Phys. **81**, 2384 (1997).
- ¹³D. C. Paine, C. Caragianis, T. Y. Kim, Y. Shigesato, and T. Ishahara, Appl. Phys. Lett. **62**, 2842 (1993).
- ¹⁴M. Nogami and Y. Abe, Appl. Phys. Lett. **65**, 2545 (1994).
- ¹⁵V. Craciun, C. Boulmer-Leborgne, E. J. Nicholls, and L. W. Boyd, Appl. Phys. Lett. **69**, 1506 (1996).
- ¹⁶B. Abeles, P. Sheng, M. D. Coutts, and Y. Arie, Adv. Phys. **24**, 407 (1975).
- ¹⁷E. Šimánek, Solid State Commun. **40**, 1021 (1981).
- ¹⁸P. Sheng and J. Klafter, Phys. Rev. B **27**, 2583 (1983).
- ¹⁹G.-F. Hohl, S. D. Baranovskii, J. A. Becker, F. Hensel, S. A. Quaiser, and M. T. Reetz, J. Appl. Phys. **78**, 7130 (1995).
- ²⁰A. L. Efros and B. I. Shklovskii, J. Phys. C **8**, L49 (1975).
- ²¹D. V. Averin, A. N. Korotkov, and K. K. Likharev, Phys. Rev. B **44**, 6199 (1991).
- ²²J. M. Ziman, J. Phys. C **1**, 1532 (1968).
- ²³M. Fujii, Y. Inoue, S. Hayashi, and K. Yamamoto, Appl. Phys. Lett. **68**, 3749 (1996).
- ²⁴Y. Kanzawa, S. Hayashi, and K. Yamamoto, J. Phys.: Condens. Matter **8**, 4823 (1996).
- ²⁵S. Hayashi, M. Kataoka, and K. Yamamoto, Jpn. J. Appl. Phys., Part 2 **32**, L274 (1993).
- ²⁶S. Hayashi, M. Kataoka, Y. Kanzawa, and K. Yamamoto, Proceedings of the 22nd International Conference on the Physics of Semiconductors, 1995, p. 2023.